



Contents lists available at ScienceDirect

Fire Safety Journal

journal homepage: <http://www.elsevier.com/locate/firesaf>

In-situ measurement of water-vapor in fire environments using a real-time tunable diode laser based system

Shruti Ghanekar^a, Rajivasanth Rajasegar^a, Nicholas Traina^a, Constandinos Mitsingas^a, Richard M. Kesler^b, Gavin P. Horn^{b,c}, Robin Zevotek^c, Stephen Kerber^c, Tonghun Lee^{a,*}

^a Department of Mechanical Science and Engineering, University of Illinois, Urbana, IL, USA

^b Illinois Fire Service Institute, University of Illinois at Urbana-Champaign, 11 Gerty Drive, Champaign, IL, 61820, USA

^c UL Firefighter Safety Research Institute, 6200 Old Dobbin Ln. Suite 150, Columbia, MD, USA

ARTICLE INFO

Keywords:

Tunable diode laser
Near-infrared
Absorption spectroscopy
Water-vapor measurement
Training fires
Fire suppression
Smoke obscuration

ABSTRACT

A robust tunable diode laser absorption spectroscopy (TDLAS) based system is developed and deployed to make real-time water-vapor concentration measurements in quasi-controlled live-fire experiments conducted in firefighter training props. This system targets the 1392.5 nm (7181.15 cm^{-1}) water-vapor absorption line while employing a multi-tier detection sensitivity scheme that allows for measurements at multiple locations in fire environment through varying smoke obscuration levels. Temperature-corrected absorbance values are compared to HITRAN simulations to quantify water-vapor concentration. Upon validation in laboratory setting, the impact of firefighter hose stream application on water-vapor concentration is studied. Comparative effects of training structures (metal, concrete and drywall-lined) and fuel-loads (pallet/straw, lightweight furnishings and pallet/straw/oriented-strand-board (OSB)) on water-vapor concentration are characterized. Despite small increase in water-vapor concentration due to suppression, the post-suppression concentrations are found to be comparable or lower than the corresponding maximum pre-suppression concentrations in all scenarios except the metal structure. Irrespective of the structure, highest temperature and water-vapor concentrations are measured with pallet/straw/OSB fuel-load. Under identical fuel-loads, the drywall structure scenarios generate highest water-vapor concentration. Peak water-vapor concentrations are measured post-suppression in typical training structures (near-floor and crawling levels), but prior to suppression in the structure/fuel package combination that simulated a typical residential fire scenario.

1. Introduction

There exists a complex interplay between water and fire. Water is a primary byproduct in the combustion of hydrocarbon materials such as those that are common fuels in unwanted structure fires in the built environment. At the same time, water is the primary suppression agent used by firefighters to combat Class A fires. Fire service application of water is critical for successful and safe fire extinguishment. If not applied in appropriate flow rate, nozzle pattern and location, suppression streams may not reach the source of the fire and/or result in the generation of excess steam, potentially endangering occupants of the structure and the firefighter themselves. In recent years, there has been a conscious scientific effort geared towards understanding fires in terms of the underlying parameters: temperature, pressure, heat flux, concentrations of chemical species –oxygen, carbon dioxide, carbon monoxide,

etc. [1–4]. However, the relative magnitude of moisture introduced into the environment by steam production from application of water to a burning fuel compared to that generated by the fire itself is not well understood. In fact, the ability to measure moisture at elevated temperatures has been identified as a need for improved hazard assessments for occupants who are potentially trapped in the structure. In the SFPE Handbook [5], Purser suggests that: "... it is possible that the presence of water-vapor may be an important neglected hazard in fires." and "Humid air, steam or smoke with a high thermal capacity of latent heat (due to vapor content or suspended liquid or solid particles) may be dangerous at temperatures of around 100 °C, causing burns throughout the respiratory tract."

The ability to measure moisture concentration in such environments is a critical tool for research in firefighter safety as well as to fully understand the impact of tactical decisions on trapped occupants' safety.

* Corresponding author.

E-mail address: tonghun@illinois.edu (T. Lee).

<https://doi.org/10.1016/j.firesaf.2020.103114>

Received 15 January 2020; Received in revised form 30 March 2020; Accepted 28 April 2020

Available online 4 May 2020

0379-7112/© 2020 The Authors.

Published by Elsevier Ltd.

This is an open access article under the CC BY-NC-ND license

(<http://creativecommons.org/licenses/by-nc-nd/4.0/>).

While several instruments exist to characterize parameters such as temperature, heat flux and gas concentrations in a fire environment within a structure, the ability to measure moisture content in conditions applicable to describing fire environments, particularly after application of water to suppress the fire is a challenging issue. The amount of moisture content in an environment can be derived from humidity measured using instruments such as psychrometers, optical condensation hygrometers and dew cells which record dew point of the sample or from measurement of the change in electrical properties of certain hygroscopic materials that respond to changes in relative humidity. Most of these techniques are not suitable for moisture measurements at high temperatures. Although chilled mirror hygrometers which measure the dew point are used in high temperature commercial furnace environments and capacitive hygrometers have been used to make water-vapor measurements in prescribed grass fire, smoldering smoke and biomass combustion plumes [6–8], these instruments have a slow response time and are incapable of measuring water-vapor concentration as percentage of air. Moreover, sampling gases at high temperatures for transport for remote moisture measurements is challenging due to the need for bulky and cumbersome techniques to prevent condensation before it reaches the instrument. It is likewise impractical to sample and condense water-vapor to get a percentage of water-vapor in air at a sampling resolution of 1 Hz in a full-scale out-of-laboratory experiment. A more direct approach can be adopted to measure moisture content *in situ* using a spectroscopic technique such as tunable diode laser absorption spectroscopy (TDLAS), in which the amount of absorbed light at a particular wavelength is directly proportional to the moisture content in the environment. As the measurement is carried out by using a beam of laser across the medium, an apparatus to prevent condensation in the sampling lines is not required. Furthermore, this technique allows for accurate, continuous, *in situ* measurements without affecting the species composition at the measurement location.

TDLAS techniques are often used to measure species concentration in high-temperature and high-pressure reactive environments such as combustors and shock tubes [9–15] as well as in harsh environments such as furnaces, power plants and boilers where obscuration presents a major challenge to the successful measurement of the species concentration [16–23]. Tunable diode laser absorption techniques have also been successfully used to make *in situ* molecular oxygen concentration measurements in fire environments, where varying levels of obscuration due to smoke and elevated temperatures present a serious challenge [24, 25].

In addition to the scientific utility of this tool, such an instrument can be valuable for informing and training firefighters on the impact of hose stream application. A common concern in the US Fire Service is the impact of fire streams on occupant tenability, particularly with respect to steam generation and the risk for trapped occupant burns [26]. Firefighters are taught about hose stream application – and often steam generation – during live-fire training scenarios that are typically conducted in structures with concrete or metal walls using wood-based fuels such as pallets and/or engineered wood products such as oriented strand board (OSB). However, typical residential fires are suppressed in structures with drywall surface finishes and largely polymer-based fuels. If the feedback from the training fire environment does not appropriately simulate typical residential structure fires, an incorrect message may be reinforced to the firefighters.

In this work, development and laboratory assessment of a multi-tier TDLAS system is described first. This tool is then applied to a series of quasi-controlled experiments conducted at the Illinois Fire Service Institute (IFSI) using three types of fuel loads in three different training props. Changes in water-vapor concentration are characterized as the fire evolves and is suppressed by hose stream water application.

2. Tunable diode laser absorption spectroscopy

For this application, a water-vapor measurement system based on

tunable diode laser absorption spectroscopy (TDLAS) technique can provide a path averaged point measurement of water-vapor concentration as per Beer-Lambert's law defined in Eq. (1) [27]. For any medium described by total pressure, P and temperature, T , assuming the losses due to light scattering are negligible the absorbance, A_ν is given by

$$A_\nu = -\log_{10}\left(\frac{I}{I_0}\right)_\nu = \log_{10}(e)k_\nu L = \log_{10}(e)\frac{pL}{kT}Sg_\nu \quad (1)$$

where I_0 is the intensity of incident light and I is the intensity of transmitted light $k_\nu L$ is the optical depth of the medium. S ($\text{cm}^{-1}/(\text{molecule}/\text{cm}^2)$) is the spectral line intensity, g_ν ($1/\text{cm}^{-1}$) is the spectral line shape and k is the Boltzmann's constant. Partial pressure, p (atm) of the absorbing species is the product of the volume mixing ratio, q and total atmospheric pressure, P . The spectral absorption coefficient, k_ν at wavenumber ν is defined as

$$k_\nu = \frac{qP}{kT}Sg_\nu \quad (2)$$

The calculated absorbance is then compared to simulated absorption spectrum based on parameters obtained from the HITRAN database. The HITRAN molecular absorption database is a compilation of spectroscopic parameters that can be used to predict and simulate absorption and emission of 49 species in the visible, infrared and microwave region of the electromagnetic spectrum. In our current setup, water-vapor concentration p , expressed as percentage of water-vapor of air by volume (partial pressure x 100%), is calculated based on experimental parameters I_0 , I , P , T and L , and parameters S and g_ν calculated from the HITRAN database [28], using equations adopted from Ref. [29].

3. Sensor design

The water-vapor measurement system developed at University of Illinois at Urbana-Champaign employs a three-tier sensitivity scheme. The absorption line at 1392.5 nm (7181.15 cm^{-1}) in the vibrational overtone band of water-vapor is targeted for use in the TDLAS based water-vapor measurement system. This line's isolation, verified using the HITRAN database, from the absorption spectra of the other gaseous species present in the combustion environment such as CO_2 , CO , O_2 , C_2H_2 , CH_4 , HCHO , HCN , N_2 , etc. and liquid water and its high line strength up to $650 \text{ }^\circ\text{C}$, and the readiness and availability of an inexpensive laser source on the market makes this line an ideal target for the sensor. Atmospheric water-vapor measurements and measurements in shock tunnels and subsonic jets have been carried out by targeting this particular line [30–34].

A 15-mW single mode tunable diode laser (Eblana Photonics, EP1392-5-DM series) with a center wavelength of 1392 nm is used as the laser source. The laser is scanned in wavelength by using a saw-tooth modulation of the bias current using a laser controller (Arroyo Instruments, 6305) which has an inbuilt temperature controller which maintains the laser's temperature using a thermoelectric cooler (TEC) integrated with the laser diode mount (Arroyo Instruments, 203). To carry out simultaneous water-vapor concentration measurements at three different locations, the diode laser output is split into four beams of equal intensity using a 1x4 (25:25:25:25) wideband fiber optic coupler (Thorlabs, TNQ1300HF), of which three outputs are used. Custom length fiber optic patch cables (Thorlabs, SMF-28-J9) are used for transmitting the laser beam to and from the measurement location where it is pitched across a pre-set path length and caught using FiberPort collimators (Thorlabs, PAF2P-11C). The FiberPort collimators are fitted with uncoated calcium fluoride (CaF_2) 30 arcmin wedge windows (Thorlabs, WW51050) to protect the collimation optics from soot and other corrosive species present in the fire environment. A K-type thermocouple (Omega, 5SRTC-GG-K-24-36) with bead diameter of 0.6 mm and response time of 0.84 s is deployed with each collimator to measure local temperature.

Each laser beam transmitted back from the measurement location is successively split using two 99:1 fiber optic couplers (Thorlabs, TW1300R1F1) as shown in Fig. 1(a), to form a three-tier sensitivity scheme that allows measurement from 0.01% light transmission (heavy smoke) to 100% light transmission (no smoke) conditions. Suitable combinations of optical attenuators (Thorlabs, FA03T, FA05T, FA10T) are used to ensure smooth transitions between sensitivity levels which were verified by two-compartment (fire room, target measurement room) table top smoke box test. Three InGaAs fixed gain amplified photodiodes (Thorlabs, PDF10C) are used to detect the laser beam transmitted from each measurement location. The photodiode (intensity) and thermocouple (temperature) outputs are continuously recorded throughout the duration of an experiment using a National Instruments (NI) data acquisition (DAQ) system and a LABVIEW interface at a sampling frequency of 1 Hz. The total pressure is assumed to be 1 atm throughout the experiment while the path length is fixed at 3.88 cm. The program simultaneously processes the photodiode and thermocouple signals to provide real-time water-vapor measurements. The DAQ system is also used to simulate a 1 Hz sawtooth waveform that serves as input to the laser controller which modulates the laser’s optical output in both intensity and wavelength, thus providing a ‘wavelength scan’ required for performing TDLAS measurements.

For each measurement at each location, the LABVIEW program is capable of selecting the least saturated non-zero voltage level, I , from the three acquired photodiode signals and then fit a linear baseline to I , which represents the intensity of incident light, I_0 . This procedure is shown in Fig. 1(b) with the transmitted intensity, I in blue and incident intensity, I_0 in red for one wavelength scan performed at 1 Hz. The double horizontal (X-axis) scale is used to correlate the temporal modulation (time in seconds) of the laser output to its corresponding wave number (cm^{-1} , inverse of wavelength). Estimating the incident intensity for each data point separately eliminates the effects of scattering by particulates or any potential thermal induced misalignment of the optics that may attenuate signal over the entire range of wavelength scanned, such that these sources of variability should have no impact on the water-vapor measurements. I_0 estimation by fitting a linear baseline for two data points with different levels of smoke obscuration is shown in Fig. 1(c). A distinct drop in transmitted intensity is seen at 1392 nm (7181.15 cm^{-1}) in both cases, with obscuration (data2) and without (data1). The absorbance is calculated using Eq. (1). The measured peak absorbance is then iteratively compared with calculated peak absorbance values from the simulated absorption spectrums based on the HITRAN database at the measured temperature. To reduce the processing time, a matrix of peak absorbance values for water-vapor partial

pressures ranging from 0 to 0.5 atm in steps of 0.01 atm and temperatures ranging from $-23.15 \text{ }^\circ\text{C}$ (250 K) to $526.85 \text{ }^\circ\text{C}$ (800 K) in steps of $1 \text{ }^\circ\text{C}$ for the set path length of 3.88 cm (1.53 in) is obtained beforehand. When necessary, a linear interpolation scheme is implemented to estimate the corresponding partial pressure at a given temperature.

For validating the accuracy of the water-vapor measurement system, an environmental chamber (Tenney, T20RS) located at IFSI whose temperature and relative humidity (RH) can be closely controlled was used. Table 1 shows the comparison between the RH settings of the environmental chamber and the corresponding RH values calculated based on vapor pressure equation (Eq. (3)), from the measured water-vapor concentration using the water-vapor measurement system.

$$\ln\left(\frac{p_\sigma}{p_c}\right) = \frac{T_c}{T} (a_1\vartheta + a_2\vartheta^{1.5} + a_3\vartheta^3 + a_4\vartheta^{3.5} + a_5\vartheta^4 + a_6\vartheta^{7.5}) \quad (3)$$

where p_σ is the vapor pressure in MPa, $\vartheta = (1 - T/T_c)$, $T_c = 647.096 \text{ K}$, $p_c = 22.064 \text{ MPa}$, $a_1 = -7.859 517 83$, $a_2 = 1.844 082 59$, $a_3 = -11.786 649 7$, $a_4 = 22.680 741 1$, $a_5 = -15.961 871 9$, and $a_6 = 1.801 225 02$ [35].

In a typical dataset, the water-vapor concentration is measured using the highest sensitivity level (level 3) with lowest laser power until well after ignition in relatively low smoke conditions. The other two sensitivity levels are fully saturated. As the smoke layer starts to descend at the measurement location, obscuration due to smoke increases resulting in decrease in the intensity of transmitted laser beam. As it is no longer possible to make water-vapor measurements using sensitivity level 3, signal from sensitivity level 2, which has higher power is used. In case of heavy smoke obscuration, signal from sensitivity level 1 is selected to make water-vapor measurements as the power from sensitivity level 2 is insufficient. Data from all three sensitivity levels is recorded and the appropriate signal is used for data analysis thereby providing continuous water-vapor concentration measurement throughout an experiment.

Table 1
Environmental chamber RH readings compared to calculated RH values.

| Temperature ($^\circ\text{C}$) | Chamber RH reading (%) | Measured partial pressure of water-vapor (%) | Calculated RH (%) | Error in calculated RH (%) |
|----------------------------------|------------------------|--|-------------------|----------------------------|
| 35.0 | 6.00 | 2.68 | 6.34 | 5.67 |
| 35.0 | 35.0 | 1.91 | 34.9 | 0.31 |
| 35.0 | 64.0 | 3.57 | 64.6 | 0.95 |

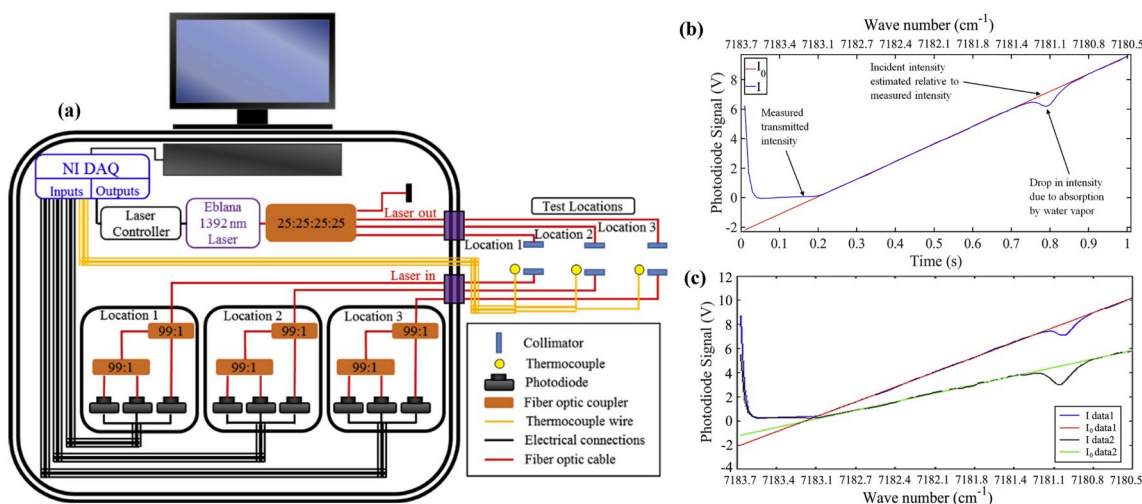


Fig. 1. (a) Schematic layout of the TDLAS based water-vapor measurement system, (b) Estimation of incident intensity I_0 , based on transmitted intensity I . (c) Effect of obscuration on measurement.

4. Training fires – Experimental setup

Traditionally, recruit firefighters are often trained in live-fire scenarios in buildings constructed of concrete, where natural fuels such as pallets and/or straw are ignited in one section of the room. The resulting fire does not develop into a fire similar to that fueled by common household furnishings. Moreover, the fire does not respond in a similar fashion to ventilation and fire service interventions like today's compartment fires. Hence, there is a concern that training fires can result in unrealistic visual cues and fire behavior that is markedly different from what could be experienced in the field under similar conditions. Lately, many firefighter training academies are using metal containers to replace or supplement their concrete training buildings. The metal training props are much less expensive up front and the containers can be combined into various geometries with relative ease, can be reconfigured and refurbished by cutting and replacing the individual containers. However, it is crucial to note that the growth, evolution and response of the fire to suppression and ventilation tactics can have important differences between the residential building structures, concrete structures and metal structures due to their dissimilar properties [36].

While structural and ventilation characteristics differ between residential structures and those used for live-fire training, there is also a significant difference in the type, quantity and configuration of fuel used. The fuel load in modern residential occupancies is typically considerably higher than the one that is typically used in live-fire training. In the United States, pallet and straw or pallet and straw with oriented strand boards (OSB) are the typical fuel loads used for training fire scenarios while a major portion of the fuel load in residential fires are the furnishings [36].

To compare and contrast the moisture concentrations during the evolution and suppression of fire in three structures commonly used for firefighter training, i.e., metal structures made from shipping containers, concrete structures and gypsum drywall lined wooden structures, a series of experiments are conducted at the University of Illinois Fire

Service Institute, Champaign, IL with the fuel loads shown in Fig. 2(a,b,c) and existing structures with layouts shown in Fig. 2(d,e,f) that are used by IFSI to routinely train firefighters. Following in UL FSRI's report *Evaluation of the Thermal Conditions and Smoke Obscuration of Live Fire Training Fuel Packages* [37], the pallet and straw configuration used in these experiments is similar to 3P1S-V configuration (peak heat release rate (HRR) = 2.0 MW [37]) while the pallet, straw and OSB fuel load is similar to 3P1SO configuration (peak HRR = 2.4 MW [37]), though included variations in the OSB panel orientation to fit within the training structure environment. The barrel chair used in these experiments is identical to BC-1 as described (peak HRR = 0.85 MW [37]). The fuels were stored in a dry outdoor location prior to utilization in the training scenarios as is common in fire training academies. Although the fuel load moisture content is not controlled or assessed, it is expected to be consistent across the scenarios. While the UL report provides information on fuel weights and heat release rates, it should be noted that the fuel burning characteristics may have deviated from those obtained in a free burn under a laboratory hood in the report, due to confinement within the training structures and suppression before complete consumption of the fuel load.

For each of the nine structure and fuel load combinations, water-vapor concentration and temperature is measured at three different heights: 0.3 m, 0.9 m and 1.5 m from the floor. The height of 0.3 m from the floor approximates the location of a trapped occupant lying on the floor, while 0.9 m would be similar to an occupant sleeping on the bed or crawling on the ground and the height of 1.5 m would correspond to a person in a standing posture. The water-vapor concentration measurements are made at the location from where a firefighter would normally apply water streams during training evolutions as this is the location where the student will sense changes in environment during suppression. Table 2 identifies the fuel loads, containment structure and the sequence of events (ignition, suppression and ventilation) in the series of experiments.

For each scenario, the fuel load is placed in the bedroom furthest away from the entrance and the water-vapor measurement system is



Fig. 2. Fuels used for experiments (a) Pallet and straw, (b) Pallet, straw and OSB, (c) Barrel chair as a representative of lightweight furnishing. Layouts of structures used for experiments (d) Concrete structure, (e) Metal structure, (f) Drywall structure commonly used for training firefighters at IFSI. The measurement location (green boxes) and the location of fuel load ignition (flames) are marked on the layouts. Unused sections of the structures are indicated by dark grey. (For interpretation of the references to colour in this figure legend, the reader is referred to the Web version of this article.)

Table 2

Details of the experiments and event times recorded after start of data acquisition.

| Structure | Fuel | Ignition (mm:ss) | Suppression (mm:ss) | Ventilation (mm:ss) |
|-----------|------------------------|------------------|---------------------|---------------------|
| Metal | Pallet and Straw | 2:00 | 8:30 | 11:30 |
| Metal | Pallet, Straw and OSB | 2:00 | 8:30 | 10:30 |
| Metal | Lightweight Furnishing | 2:30 | 9:00 | 11:30 |
| Concrete | Pallet and Straw | 2:00 | 8:30 | 10:30 |
| Concrete | Lightweight Furnishing | 2:30 | 6:30 | 8:30 |
| Concrete | Pallet, Straw and OSB | 2:45 | 9:15 | 10:15 |
| Drywall | Pallet and Straw | 2:00 | 8:30 | N/A |
| Drywall | Lightweight Furnishing | 2:00 | 8:30 | N/A |
| Drywall | Pallet, Straw and OSB | 2:00 | 8:30 | N/A |

placed near the doorway between the target room and the fire room but protected from direct radiant heat from the fire. The location is slightly different in each structure due to the varying layouts but is chosen to be as close as possible to the location where firefighter trainees apply suppression streams into the fire room. The fuel load is ignited using handheld emergency flares and ignition is confirmed visually. As is typical in live-fire training, the windows of the fire room are sequentially closed to contain the smoke inside the structure in an effort to control the visual obscuration levels during the experiments. At six and half minutes after ignition, suppression streams are applied directly to the burning fuels by firefighting crew using a 1¼ inch manual firefighting handline with a combination nozzle on the tight straight stream setting with typical flow rate of 200–300 L per minute (~50–80 gallons per minute) until the fire is fully suppressed in less than 10 s. The target suppression time was determined as the time when highest temperature was recorded in a separate series of experiments. Approximately 2 min after suppression, the doors and windows are opened to let the smoke exit the structure and cool down.

5. Data, results and discussion

The percent of water-vapor in the atmosphere near the Earth's surface undergo both seasonal and diurnal variations [38,39]. As the experiments are conducted outside of a controlled laboratory

environment, it is necessary to record the water-vapor concentration in the ambient air prior to each scenario. Doing so allows for comparison between water-vapor generated by the fire and suppression regardless of the location and time when the experiment is conducted. Therefore, for each experiment, the background is recorded for at least 2 min, at the end of which the fuel load is ignited. After ignition, both the temperature and water-vapor concentration are observed to increase until the fire is suppressed by application of water directed at the burning fuel load. The effect of the suppression event is almost immediate on both the measured temperature and water-vapor concentration at the 1.5 m height as it is most directly in contact with the smoke layer. After about 2 min, as the structure is ventilated both the temperature and water-vapor concentration decrease as the cooler and drier air enters the structure from outside.

A typical water-vapor measurement dataset is presented in Fig. 3 with the automatically selected laser measurement sensitivity level overlaid. The events of ignition, suppression and ventilation are marked. The measurement system's ability to measure water-vapor concentration continuously through varying levels of smoke obscuration using the three-tier sensitivity scheme is demonstrated. Line-averaged local measurements carried out at the sensor location are assumed to be indicative of the overall water-vapor concentration at that selected height. However, it is critical to analyze the temporal evolution of water-vapor by focusing predominantly on the large-scale dynamics (global, on the order of tens of seconds) as the small-scale fluctuations (local, on the order of few seconds) in water-vapor concentration may partly be due to localized effects such as a strong directional draft driving hot gases/smoke/vapor cloud momentarily into the sensor's probe volume. Furthermore, some of the repetitive, rapid and abrupt fluctuations (10–15% change within few seconds) observed in the measured water-vapor concentration (highlighted in yellow in Fig. 3) may partly be due to the changes in the sensitivity tier. The standard error (normalized with respect to the mean) in water-vapor concentration measurements is estimated to be less than 1% calculated based on the measured water-vapor concentration in ambient air. This assumes homogeneity in temperature and composition within the path length. However, even due to the largest thermal stratification observed in the vertical direction at a measurement location (gradient of 334 °C/1.2 m for pallet, straw and OSB scenario in concrete structure), the estimated temperature variation over the path length is about 10 °C which translates to a relative error (variation) of less than 3% in the measured water-vapor concentration.

The results from the nine experiments are presented in Fig. 4 for metal structure, in Fig. 5 for concrete structure and in Fig. 6 for drywall

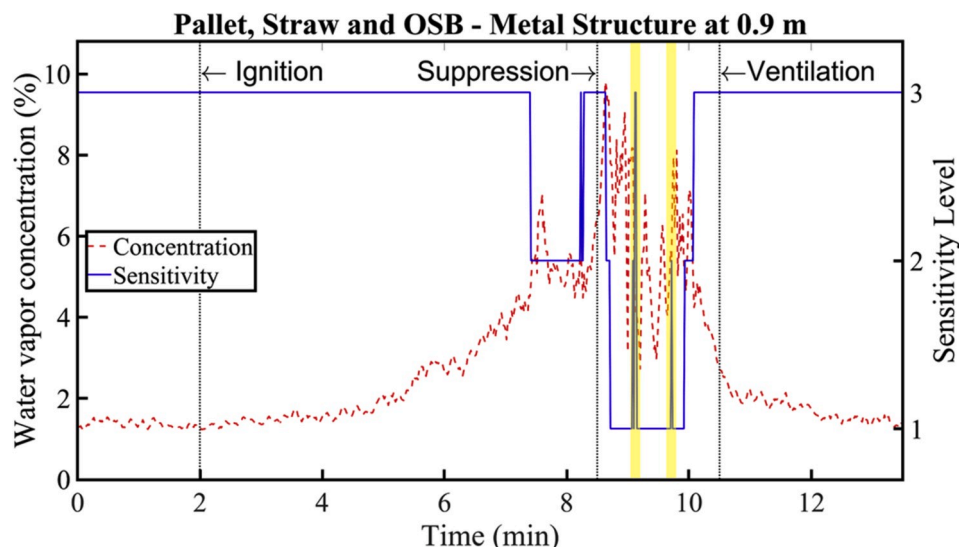


Fig. 3. A dataset showing continuous water-vapor measurement using various sensitivity levels.

structure. The top sub-panel shows the time evolution of temperature and bottom sub-panel shows time evolution of water-vapor concentration in each panel of all the three figures. The traces in green are measurements at the height of 1.5 m, in red are at the height of 0.9 m and in blue are at the height of 0.3 m above the floor. Panel (a) of all the figures presents data from experiments with pallet and straw, panel (b) from experiments with pallet, straw and OSB and panel (c) from experiments with lightweight furnishings as fuel load. The ignition, suppression and ventilation events are marked by vertical lines. It can be clearly seen that at the measurement height of 1.5 m from the floor, the highest temperatures and water-vapor concentrations are observed. Finally, Fig. 7 summarizes the background and maximum water-vapor concentrations before and after the suppression event for the three fuel loads in the three structures at 1.5 m in panel (a), 0.9 m in panel (b) and 0.3 m in panel (c). The labels on each bar indicate whether the overall maximum concentration is recorded before or after the suppression event in each experiment at each height.

In the same structure, temperatures recorded in experiments with pallet, straw and OSB are consistently the highest followed by experiments with lightweight furnishings while lowest temperatures are recorded in experiments with pallet and straw. For experiments with pallet and straw as fuel load a temperature spike shortly after ignition is observed as the straw rapidly ignites and spreads to the pallets, followed by multiple smaller peaks and valleys with a general decreasing trend. For experiments with lightweight furnishing as fuel load, two distinct temperature peaks are observed in metal and drywall structures. In the concrete structure, the fire is suppressed only 4 min after ignition as opposed to 6 min in the other structures. For experiments with pallet, straw and OSB as fuel load, temperature is observed to increase, and it remains relatively high until suppression. Multiple local peaks in temperature observed during fire evolution are most likely caused due to differences in heat release rates of various fuel load components owing to their dissimilar chemical compositions. In all cases, a pronounced drop in temperature is observed after suppression. Ventilation causes the temperature to return to about 10 °C higher than the background level at

0.9 m and 0.3 m and about 20 °C higher than background at 1.5 m.

Each training structure also displays important differences in fire development. For the metal structure, the temperature increase is observed after about 3 min after ignition and the increase is gradual while, in case of concrete and drywall structures, a spike in temperature is observed about 1 min after ignition. The temperatures recorded in the metal structure are consistently lower than the temperatures recorded in concrete and drywall structures by about 100–250 °C. The higher thermal conductivity of the metal structure (steel: 8.7 to 66 Wm⁻¹K⁻¹) would result in a higher heat loss to the surroundings than in concrete or drywall structure (concrete: 0.1 to 0.7 Wm⁻¹K⁻¹, gypsum board: 0.17 Wm⁻¹K⁻¹) [40,41]. After suppression the temperature plummets in the concrete and drywall structures while a gradual decrease is observed in the experiments conducted in the metal structure.

The background water-vapor concentrations are recorded in the range of 1%–2.3% for the various experiments. As expected, an increase in the water-vapor concentration is observed as the fire evolved. In the metal structure, the water-vapor concentrations begin to increase at a longer time after ignition compared to the other structures, regardless of the fuel package. This delay in smoke filling the compartment is in part due to higher leakage from the metal structure and dissimilar structure layouts and measurement location placement relative to fuel loads. While these differences are common in typical live fire training structures, these factors must be taken into consideration while comparing water-vapor concentrations between the various structures. Higher water-vapor concentrations are recorded at greater height from the floor, closer to the smoke layer in the target room. The maximum water-vapor concentration at 1.5 m and 0.3 m is observed before suppression to be 41.7% and 4.46% respectively in drywall structure with pallet, straw and OSB as fuel load. However, somewhat surprisingly, at 0.9 m from the floor, maximum concentration of 9.8% is recorded after suppression in the metal structure with pallet, straw and OSB as fuel load.

For a given structure, water-vapor produced during the fire evolution phase in experiments with pallet and straw is the lowest followed by water-vapor produced with lightweight furnishings while experiments

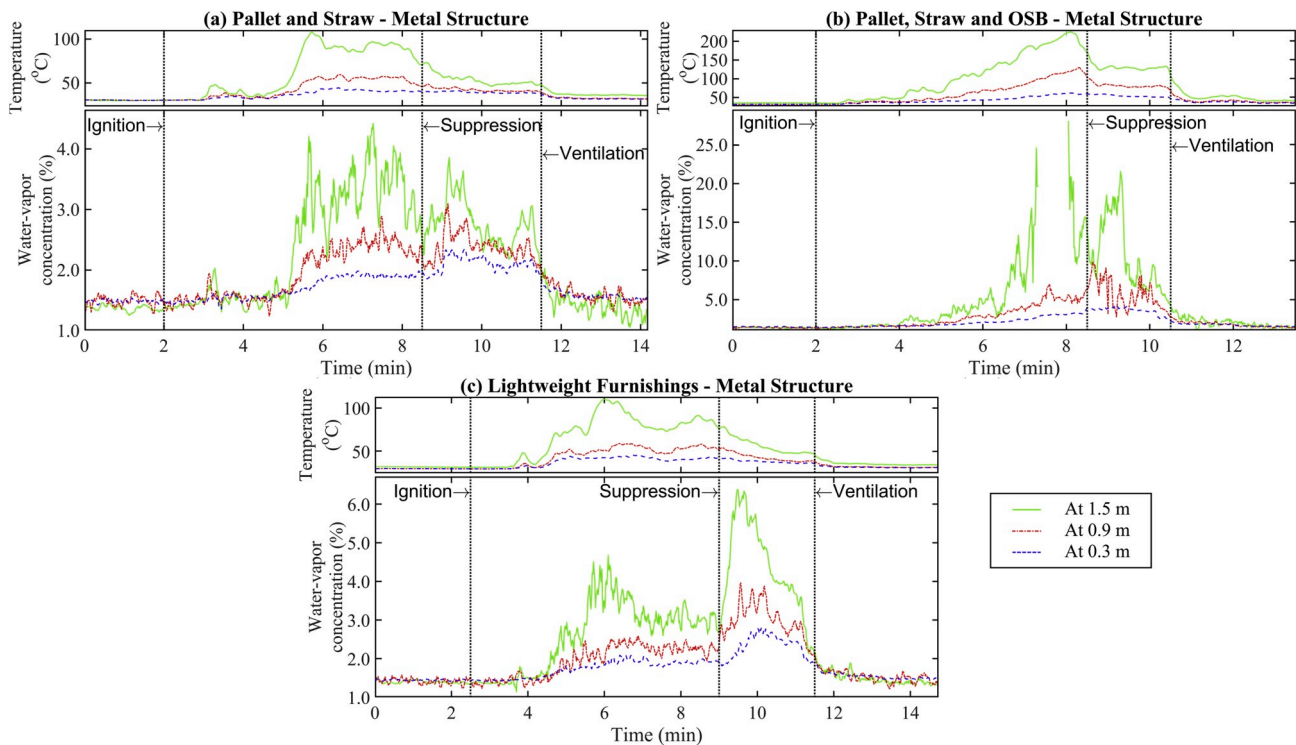


Fig. 4. Temperature and water-vapor concentration plots for experiments in metal structure with (a) Pallet and straw, (b) Pallet, straw and OSB and (c) Lightweight furnishings.

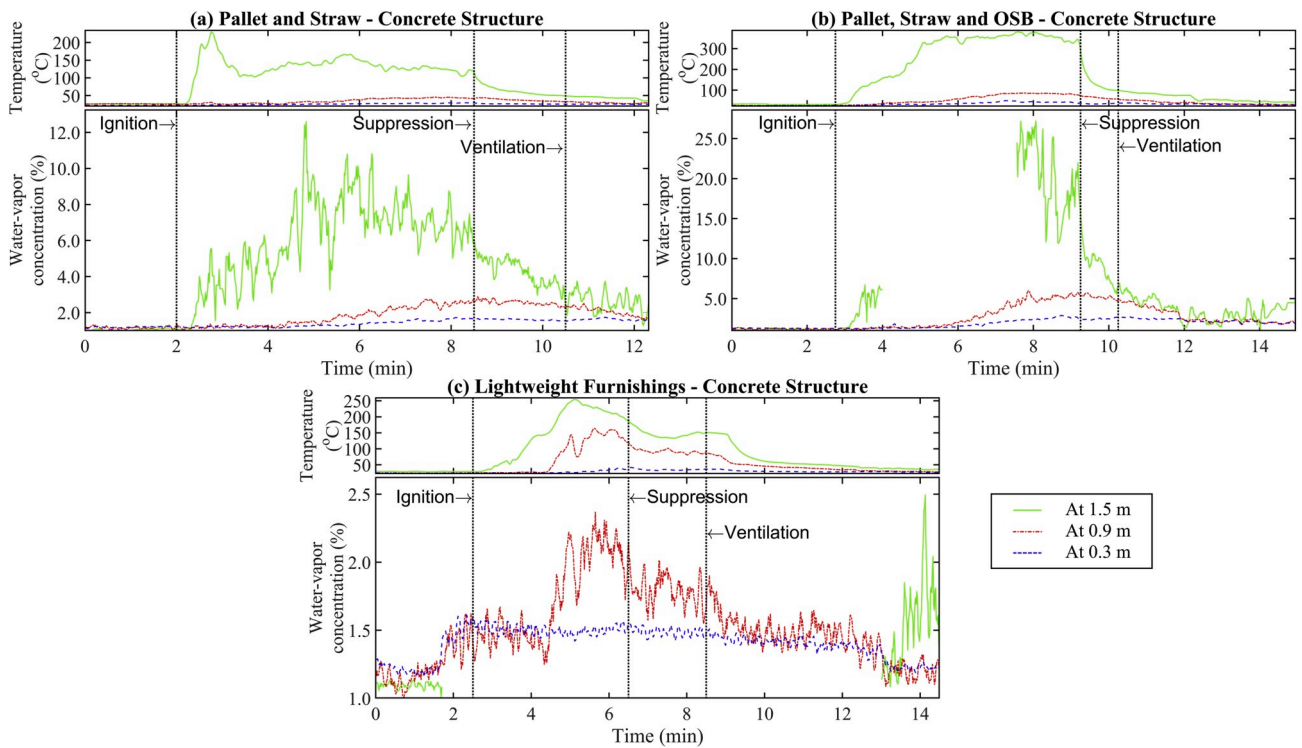


Fig. 5. Temperature and water-vapor concentration plots for experiments in concrete structure with (a) Pallet and straw, (b) Pallet, straw and OSB and (c) Lightweight furnishings.

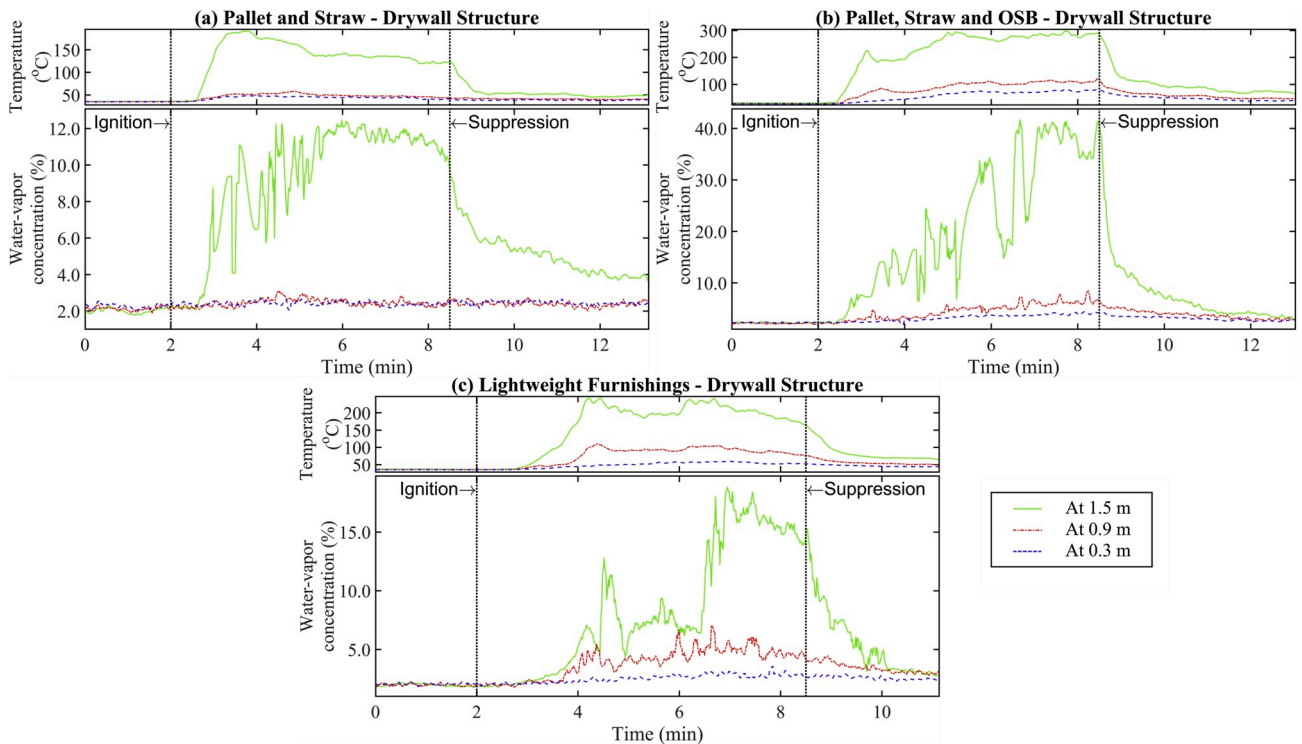


Fig. 6. Temperature and water-vapor plots for experiments in drywall structure with (a) Pallet and straw, (b) Pallet, straw and OSB and (c) Lightweight furnishings.

with pallet, straw and OSB as fuel load produce the highest water-vapor during fire evolution. During the development phase, fires with pallet and straw produce water-vapor almost uniformly throughout fire evolution after the initial post-ignition spike during straw combustion. Training fires with pallet, straw and OSB as the fuel load result in water-

vapor concentration generally increasing from ignition until suppression. In experiments with lightweight furnishings, multiple distinct spikes in water-vapor concentration are observed before suppression owing to different components of the fuel load being consumed at different rates. Despite the three-tier sensitivity scheme, experiments

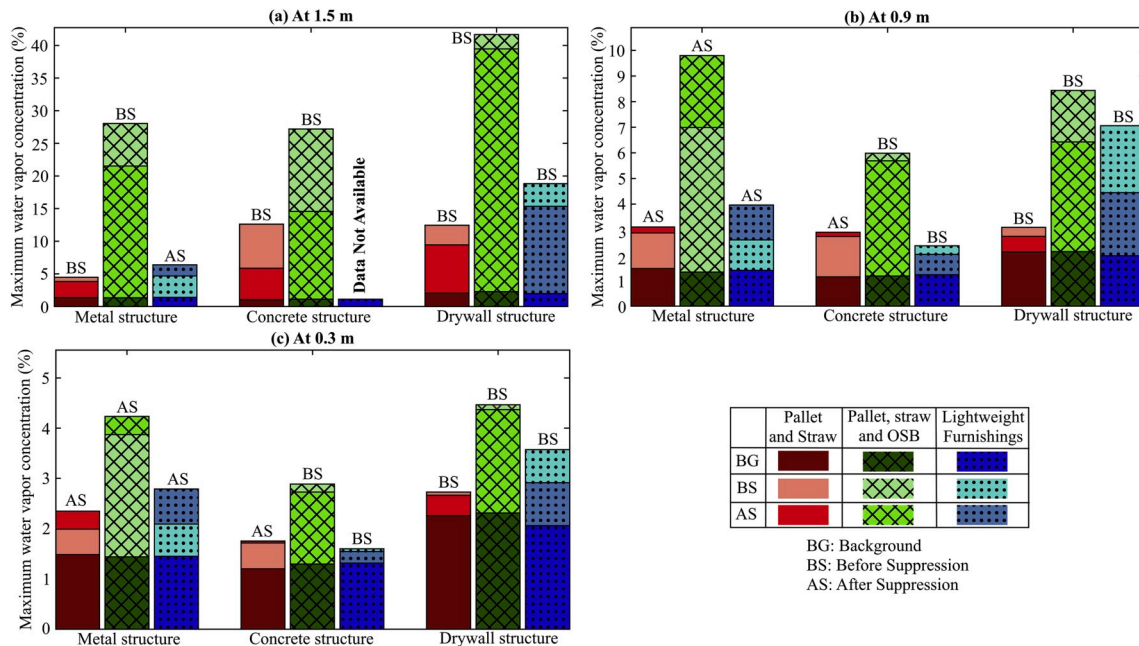


Fig. 7. Comparison of maximum water-vapor concentrations in the three structures for pallet and straw (plain), pallet, straw and OSB (cross-hatched), and lightweight furnishings (dotted) as fuel loads at the height of (a) 1.5 m, (b) 0.9 m and (c) 0.3 m. Labels on each bar indicate whether the overall maximum concentration is observed before suppression (BS) or after (AS) suppression.

with pallet, straw and OSB fuel load in metal and concrete structures suffer loss of data at the 1.5 m height due to water-vapor condensation and heavy smoke. For lightweight furnishings as fuel load in the concrete structure, no meaningful water-vapor concentration data could be obtained at 1.5 m height due to damage to a fiber patch cable.

In concrete and drywall structures, a sharp drop in water-vapor concentration is observed after suppression at the 1.5 m height as the air temperature in the fire room drops rapidly, resulting in a decrease in water-vapor holding capacity of air (in vapor phase) causing condensation of water-vapor. Although a slight increase in the water-vapor concentration is observed in the concrete structure post suppression at 0.9 m and 0.3 m heights, the concentration is much less than that recorded pre-suppression. In contrast, in the metal structure, water application results in an increase in water-vapor concentration at all heights and the overall maximum concentration is recorded post-suppression at all heights in all experiments except for at 1.5 m height in both pallet and straw and pallet, straw and OSB scenarios.

In the drywall structure, relatively high water-vapor concentrations are observed in the pallet, straw and OSB experiment prior to suppression, with maximum water-vapor concentration of 41.7% at the 1.5 m height. In the experiment with lightweight furnishings, the water-vapor concentration increases to a maximum of 18.8% at 1.5 m height, almost three times higher than the peak measured with the same fuel load in the metal training structure. Such high concentration could most likely be attributed to gypsum ($\text{CaSO}_4 \cdot 2\text{H}_2\text{O}$) in the drywall which possibly dehydrates when subjected to temperatures above 90 °C [42]. The water-vapor concentrations at 0.9 m and 0.3 m height do not appear to be impacted by gypsum dehydration as the temperatures at those heights are typically below this threshold. For all experiments conducted in the drywall structure, the overall maximum water-vapor concentration is observed before suppression at all heights.

The difference in the layouts, ventilation conditions and the relative positions of the fuel load and measurement locations for the three structures must be taken into consideration while comparing the data presented here. The overall volume of the fire room and connected spaces, the ventilation openings and leakage paths within the structures are unique to each scenario and can influence the water-vapor concentration and the rate at which it descends towards the firefighter. The

differences in the relative placement of the sensor to the fuel load can impact comparisons between structures as discrepancies can arise as a result of mixing of the hot combustion products and steam produced after suppression with relatively cooler, dry air from the outside of the structure. It is interesting to note that the highest post-suppression changes in water-vapor concentrations are measured in the metal structure that had relatively large number of leakage paths and relatively larger distance from the fuel load to the measurement location. If these training scenarios were conducted in a smaller training structure with fewer leakage paths and the suppressing firefighter moved closer to the fire, higher levels of water-vapor may result. These differences in structural conditions are common in training firefighters in the US and should be considered by the instructor.

When taken together, these results suggest that fire instructors should use caution when training firefighters to understand changes in the post-suppression environment using typical live-fire training structures. As Fig. 7 shows, pallet and straw fires in both concrete and metal structures and OSB fueled fires in metal structures result in peak moisture concentration AFTER suppression at the 0.9 m and 0.3 m heights where trainees are likely to be operating. However, in the drywall lined structures with lightweight furnishings, peak moisture concentration is measured prior to water suppression. Water impacting hot concrete or metal components of training structures – either the walls of the metal structures or the ‘hoppers’ used to hold pallets and straw in concrete structures – can rapidly transition to steam in a manner that may not be representative of the typical residential fire environment.

6. Limitations and future work

While these live-fire training experiment represent an important early application of this water-vapor measurement system, there are important limitations to this study and valuable future work that can expand upon this paper. As discussed, the layouts and ventilation conditions for the three structures may not generalize to all training structures. Additional work can be conducted to further generalize the impact of specific training structure design elements on environmental conditions before and after suppression. Furthermore, application of this tool to full size structure fires can be important to understanding risk for

trapped occupants within a structure both pre- and post-suppression. Finally, while the three-tier sensitivity scheme provides the ability to measure moisture through a wide range of fire conditions, some data is lost at high elevations where temperatures, soot and moisture concentrations are high. Additional development of this tool may provide deeper insights into the generation and transport of this critical product of combustion.

7. Summary and conclusion

A tunable diode laser absorption-based water-vapor measurement system capable of measuring concentration of water-vapor in real time at three locations simultaneously is developed. A three-tier sensitivity scheme using various levels of laser power is implemented to acquire data through continuously changing smoke obscuration. The evolution of fire caused by burning different fuel loads in various firefighter training structures and the effect of suppression by water application at three heights in terms of temperature and water-vapor concentration at the location from where the entry team would apply water, are studied using the developed measurement system.

These initial experiments with fuels and structures used in training fires provide a unique opportunity to study the coupling between changes in air temperature and airborne water-vapor concentrations due to fires and suppression. In this study, the highest air temperatures are recorded in the concrete structure followed by the drywall structure with lowest temperatures in the metal structure (regardless of fuel load). However, the highest concentrations of water-vapor in this study are recorded in the drywall structure, followed by the concrete and metal structures. In case of drywall fire rooms, the elevated concentration of water-vapor may have been generated during the fire evolution phase due to dehydration of gypsum upon exposure to high temperature. At the same time, temperatures and water-vapor concentrations recorded in experiments with pallet, straw and OSB are the consistently the highest, followed by lightweight furnishings and pallet and straw as fuel load.

Temperature and water-vapor concentrations measured in the metal structure used in this study are quite different from those measured in the drywall structure. Both, the temperature and water-vapor concentrations recorded during the fire evolution phase are lower in the metal structure. Furthermore, water application to fires in the metal structure lead to an increase in the water-vapor concentration for all the three fuel loads at all heights in this study. The overall maximum water-vapor concentration is recorded post suppression at the heights where firefighters would be operating (0.9 and 0.3 m). Such information may be useful for firefighters and fire instructors in understanding differences in behavior between training structures and drywall lined compartments that are typical in residential fires.

Declaration of competing interests

The authors declare that they have no known competing financial interests or personal relationships that could have appeared to influence the work reported in this paper.

CRediT authorship contribution statement

Shruti Ghanekar: Data curation, Formal analysis, Investigation, Methodology, Software, Validation, Visualization, Writing - original draft. **Rajavasanth Rajasegar:** Data curation, Formal analysis, Investigation, Validation, Visualization, Writing - review & editing. **Nicholas Traina:** Conceptualization, Methodology, Software, Validation, Formal analysis. **Constandinos Mitsingas:** Methodology, Software, Validation. **Richard M. Kesler:** Validation, Investigation, Resources. **Gavin P. Horn:** Conceptualization, Funding acquisition, Investigation, Project administration, Resources, Supervision, Validation, Writing - review & editing. **Robin Zevotek:** Project administration, Funding acquisition.

Stephen Kerber: Resources, Supervision, Project administration, Funding acquisition. **Tonghun Lee:** Conceptualization, Validation, Resources, Supervision, Funding acquisition.

Acknowledgements

This work was supported by the Department of Homeland Security Fire Prevention and Safety Grant #EMW-2015-FP-00361.

References

- [1] N. Traina, S. Kerber, D.C. Kyrtsis, G.P. Horn, Occupant tenability in single family homes: Part I—impact of structure type, fire location and interior doors prior to fire department arrival, *Fire Technol.* 53 (2017) 1589–1610.
- [2] N. Traina, S. Kerber, D.C. Kyrtsis, G.P. Horn, Occupant tenability in single family homes: Part II: impact of door control, vertical ventilation and water application, *Fire Technol.* 53 (2017) 1611–1640.
- [3] K.W. Fent, D.E. Evans, K. Babik, C. Striley, S. Bertke, S. Kerber, D. Smith, G.P. Horn, Airborne contaminants during controlled residential fires, *J. Occup. Environ. Hyg.* 15 (2018) 399–412.
- [4] Kerber S. Analysis of one and two-story single family home fire dynamics and the impact of firefighter horizontal ventilation. In: *Analysis of One and Two-Story Single Family Home Fire Dynamics and the Impact of Firefighter Horizontal Ventilation*. UL Firefighter Safety Research Institute.
- [5] M.J. Hurley, D. Gottuk, J.R.J. H. K. Harada, E. Kuligowski, M. Puchovsky, J. Torero, J.M.J. W. C. Wieczorek, in: *SFPE Handbook of Fire Protection Engineering*, fifth ed., 2016.
- [6] C.B. Clements, B.E. Potter, S. Zhong, In situ measurements of water vapor, heat, and CO₂ fluxes within a prescribed grass fire, *Int. J. Wildland Fire* (2006) 299–306.
- [7] G.L. Achtemeier, Measurements of moisture in smoldering smoke and implications for fog, *Int. J. Wildland Fire* (2006) 517–525.
- [8] R.S. Parmar, M. Welling, M.O. Andreae, G. Helas, Water vapor release from biomass combustion, *Atmos. Chem. Phys.* 8 (2008) 6147–6153.
- [9] G.B. Rieker, X. Liu, H. Li, J.B. Jeffries, R.K. Hanson, Measurements of near-IR water vapor absorption at high pressure and temperature, *Appl. Phys. B* 87 (2007) 169–178.
- [10] X. Liu, X. Zhou, J.B. Jeffries, R.K. Hanson, Experimental study of H₂O spectroscopic parameters in the near-IR (6940–7440cm⁻¹) for gas sensing applications at elevated temperature, *J. Quant. Spectrosc. Radiat. Transf.* 103 (2007) 565–577.
- [11] H. Li, A. Farooq, J.B. Jeffries, R.K. Hanson, Near-infrared diode laser absorption sensor for rapid measurements of temperature and water vapor in a shock tube, *Appl. Phys. B* 89 (2007) 407–416.
- [12] J.T.C. Liu, G.B. Rieker, J.B. Jeffries, M.R. Gruber, C.D. Carter, T. Mathur, R. K. Hanson, Near-infrared diode laser absorption diagnostic for temperature and water vapor in a scramjet combustor, *Appl. Optic.* 44 (2005) 6701–6711.
- [13] A.D. Griffiths, A.F.P. Houwing, Diode laser absorption spectroscopy of water vapor in a scramjet combustor, *Appl. Optic.* 44 (2005) 6653–6659.
- [14] Z. Xin, L. Xiang, B.J. Jay, R.K. Hanson, Development of a sensor for temperature and water concentration in combustion gases using a single tunable diode laser, *Meas. Sci. Technol.* 14 (2003) 1459.
- [15] E.R. Furlong, R.M. Mihalcea, M.E. Webber, D.S. Baer, R.K. Hanson, Diode-laser sensors for real-time control of pulsed combustion systems, *AIAA J.* 37 (1999) 732–737.
- [16] Christopher R. Shaddix, S.W. A. Gary L. Hubbard, David K. Ottesen, Louis A. Gritzo, Diode laser diagnostics for gas species and soot in large pool fires, in: *Diode Laser Diagnostics for Gas Species and Soot in Large Pool Fires*. Sandia Report, SAND2001-8383, June 2001.
- [17] G.B. Rieker, *Wavelength-Modulation Spectroscopy for Measurements of Gas Temperature and Concentration in Harsh Environments*. Mechanical Engineering, Stanford University, 2009.
- [18] A. P. Melsio, W.W. Da, *Tunable diode laser for harsh combustion environments, in: Tunable Diode Laser for Harsh Combustion Environments*. Chicago IL, 2005.
- [19] L. Bergmans, J. T. Jenkins, C. Baukal, Accuracy of a Tunable Diode Laser Sensor in Large Scale Furnaces: Initial Test Results, 2005. Conference Title.
- [20] T. Jenkins, J. L. Bergmans, P. A. Debarber, M. R. Coffey, G. M. C. Starnes, I. Metrolaser, C. Ji, B. Mechatronics, M. Al, In Situ Measurements of Temperature in a Coal-Fired Power Plant Using Tunable Diode Laser Absorption Spectroscopy, 2004. Conference Title.
- [21] D. Sappey A, J. Howell, P. Masterson, H. Hofvander, J. Jeffries, X. Zhou, R. Hanson, Determination of O₂, CO, H₂O concentrations and gas temperature in a coal fired utility boiler using a wavelength-multiplexed tunable diode laser sensor, in: *Determination of O₂, CO, H₂O Concentrations and Gas Temperature in a Coal Fired Utility Boiler Using a Wavelength-Multiplexed Tunable Diode Laser Sensor*, 2004.
- [22] H. Teichert, T. Fernholz, V. Ebert, Simultaneous in situ measurement of CO, H₂O, and gas temperatures in a full-sized coal-fired power plant by near-infrared diode lasers, *Appl. Optic.* 42 (2003) 2043–2051.
- [23] T.P. Jenkins, J.L. Bergmans, Measurements of Temperature and H₂O Mole Fraction in a Glass Furnace Using Diode Laser Absorption SENSORS, IEEE, 2005.
- [24] H.E. Schlosser, J. Wolfrum, V. Ebert, B.A. Williams, R.S. Sheinson, J.W. Fleming, In situ determination of molecular oxygen concentrations in full-scale fire-

- suppression tests using tunable diode laser absorption spectroscopy, *Proc. Combust. Inst.* 29 (2002) 353–360.
- [25] H.E. Schlosser, V. Ebert, B.A. Williams, R.R. Sheinson, J.W. Fleming, NIR-diode Laser Based In-Situ Measurement of Molecular Oxygen in Full-Scale Fire Suppression Tests, 2000, pp. 492–503. Conference Title.
- [26] Zevotek R, Stakes K, Willi J. Impact of fire attack utilizing interior and exterior streams on firefighter safety and occupant survival: full scale experiments. In: *Impact of Fire Attack Utilizing Interior and Exterior Streams on Firefighter Safety and Occupant Survival: Full Scale Experiments*. UL Firefighter Safety Research Institute.
- [27] L.L. Gordley, B.T. Marshall, D. Allen Chu, Linepak: algorithms for modeling spectral transmittance and radiance, *J. Quant. Spectrosc. Radiat. Transf.* 52 (1994) 563–580.
- [28] L.S. Rothman, I.E. Gordon, Y. Babikov, A. Barbe, D. Chris Benner, P.F. Bernath, M. Birk, L. Bizzocchi, V. Boudon, L.R. Brown, A. Campargue, K. Chance, E. A. Cohen, L.H. Coudert, V.M. Devi, B.J. Drouin, A. Fayt, J.M. Flaud, R.R. Gamache, J.J. Harrison, J.M. Hartmann, C. Hill, J.T. Hodges, D. Jacquemart, A. Jolly, J. Lamouroux, R.J. Le Roy, G. Li, D.A. Long, O.M. Lyulin, C.J. Mackie, S.T. Massie, S. Mikhailenko, H.S.P. Müller, O.V. Naumenko, A.V. Nikitin, J. Orphal, V. Perevalov, A. Perrin, E.R. Polovtseva, C. Richard, M.A.H. Smith, E. Starikova, K. Sung, S. Tashkun, J. Tennyson, G.C. Toon, V.G. Tyuterev, G. Wagner, The HITRAN2012 molecular spectroscopic database, *J. Quant. Spectrosc. Radiat. Transf.* 130 (2013) 4–50.
- [29] Calculating gas spectra, in: *Calculating Gas Spectra*, 2013.
- [30] B. Parvitte, V. Zéninari, I. Pouchet, G. Durry, Diode laser spectroscopy of H₂O in the 7165–7185cm⁻¹ range for atmospheric applications, *J. Quant. Spectrosc. Radiat. Transf.* 75 (2002) 493–505.
- [31] G. Durry, N. Amarouche, V. Zéninari, B. Parvitte, T. Lebarbu, J. Ovarlez, In situ sensing of the middle atmosphere with balloonborne near-infrared laser diodes, *Spectrochim. Acta Mol. Biomol. Spectrosc.* 60 (2004) 3371–3379.
- [32] M. Brown, D. Barone, W. Terry, T. Barhorst, S. Williams, Accuracy, precision, and scatter in TDLAS measurements, in: *Accuracy, Precision, and Scatter in TDLAS Measurements*, American Institute of Aeronautics and Astronautics, 2010.
- [33] A. Al-Manea, D. Buttsworth, J. Leis, R. Choudhury, K. Saleh, Measurement of Water Vapour in Axisymmetric Jet Development Using TDLAS, 2018.
- [34] M. Kannan, Y. Krishna, G. Jagadeesh, K.P.J. Reddy, Temperature measurement in a shock tunnel using tunable diode laser absorption spectroscopy, in: A. Sasoh, T. Aoki, M. Katayama (Eds.), *Temperature Measurement in a Shock Tunnel Using Tunable Diode Laser Absorption Spectroscopy*, Springer International Publishing, Cham, 2017, pp. 395–403.
- [35] W. Wagner, A. Pruß, The IAPWS formulation 1995 for the thermodynamic properties of ordinary water substance for general and scientific use, *J. Phys. Chem. Ref. Data* 31 (2002) 387–535.
- [36] Willi J, Stakes K, Regan J, Zevotek R. Evaluation of ventilation-controlled fires in L-shaped training props. In: *Evaluation of Ventilation-Controlled Fires in L-Shaped Training Props*. UL Firefighter Safety Research Institute.
- [37] Regan J, Zevotek R. Evaluation of the thermal conditions and smoke obscuration of live fire training fuel packages. In: *Evaluation of the Thermal Conditions and Smoke Obscuration of Live Fire Training Fuel Packages*. UL Firefighter Safety Research Institute.
- [38] S. Faticchi, P. Molnar, T. Mastrotheodoros, P. Burlando, Diurnal and seasonal changes in near-surface humidity in a complex orography, *J. Geophys. Res.: Atmos.* 120 (2015) 2358–2374.
- [39] A. Dai, J. Wang, R.H. Ware, T. Van Hove, Diurnal variation in water vapor over North America and its implications for sampling errors in radiosonde humidity, *J. Geophys. Res.: Atmos.* 107 (2002). ACL 11-1-ACL 11-14.
- [40] Thermal conductivity of common materials and gases. [online], in: *Thermal Conductivity of Common Materials and Gases*, 2003 [online].
- [41] Thermal Conductivity of Metals, Metallic elements and alloys. [online], in: *Thermal Conductivity of Metals, Metallic Elements and Alloys*, 2005 [online].
- [42] G.A. Lager Ta, F.J. Rotella, J.D. Jorgensen, D.G. Hinks, A crystallographic study of the low-temperature dehydration products of gypsum, CaSO₄·2H₂O: hemihydrate CaSO₄·0.50H₂O, and γ-CaSO₄, *Am. Mineral.* 69 (1984) 910–918.